Research Report

96-29

Analytical Estimation and Reduction of Conducted EMI Emissions in High Power PWM Inverter Drives

E. Zhong, T.A. Lipo, J.R. Jaeschke*, D. Gritter*

Wisconsin Power Electronics
Research Center
University of Wisconsin-Madison
Madison WI 53706-1691

*Eaton Corporation-CORD
4201 N 27th Street Dept H503
Milwaukee WI 53216

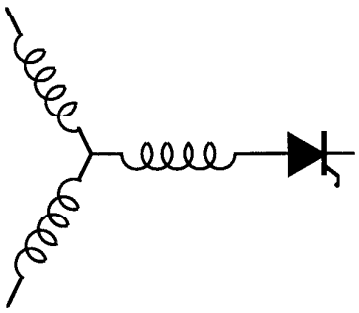

Wisconsin
Electric
Machines &
Power
Electronics
Consortium

University of Wisconsin-Madison
College of Engineering
Wisconsin Power Electronics Research Center
2559D Engineering Hall
1415 Engineering Drive
Madison WI 53706-1691

ANALYTICAL ESTIMATION AND REDUCTION OF CONDUCTED EMI EMISSIONS IN HIGH POWER PWM INVERTER DRIVES

Erkuan Zhong Thomas A. Lipo
Dept. of Electrical & Computer Engineering
University of Wisconsin-Madison
Madison, WI 53706, U.S.A
Tel: (608)262-0287

James R. Jaeschke David Gritter
Eaton Corporation-CORD
4201 N 27th St. Dept. H503
Milwaukee, WI 53216, U.S.A.
Tel: (414)449-6571

Abstract-Analytical estimation of conducted Electromagnetic Interference (EMI) from a PWM drive system is presented. Analysis of transient behavior based on a simplified circuit model of components in a drive system is performed in both the time domain and the frequency domain. The basic models of the main circuit components responding to the switching action by power devices are described. A set of EMI suppression techniques for high power drives are proposed which have been confirmed by experiment to meet the CISPR standard limits at low cost.

INTRODUCTION

PWM drive systems have been widely utilized in industrial, commercial and domestic applications due to the ease with which power can be manipulated at high efficiency. However, one of the emerging problems of static power converters is that these systems produce unwanted high frequency signals causing significant Electromagnetic Interference (EMI) [1]. New regulations governing the emissions from high power drive systems are being proposed by the IEC [2]. In previous work [1] the conducted EMI of PWM motor drives was described including measurement, explanation, and reduction of EMI emissions from an inverter-fed motor drive system rated 8 HP. In that paper, the common mode current of the pulse train flowing into the power mains was identified as the major source of conducted emission from the PWM drive system. This subsequent paper is intended to develop approaches for the analysis of the pulse train current so as to further understand origin of the noise sources and to help in EMI control. As a typical application, a set of cost-effective EMI filters for a commercial inverter of high power are introduced showing that the EMC performance of these types of drive systems is able to meet the proposed IEC standard limits at low cost.

The study of noise sources is essential in noise control. Characterization of noise is consequently the basis for comparison of methods and for filter design. There are many books, articles/papers on EMC issues addressing the EMI emission sources [3]. However approaches for quantitative prediction of noise sources is still lacking. As a basis for experimental investigation, the primary EMI noise sources of static power drive system are considered as follows:

a) first, the presented PWM signal itself, including the fundamental switching frequency, its harmonics and the side bands of the harmonics as well as its radio frquency content. The spectral content of an ideal sinusoidal control PWM wave form has been approached by Barton [4]. The spectrum of PWM signals with limited rise and falling edges has also been known to comprise a radio frequency band whose bandwidth is dependant upon the time period of edge. However, for motor drives having a switching frequency f_S of 5 kHz to 10 kHz the harmonics will shrink to a very small value over the range of hundreds of kHz so that the idealized analysis of Barton is not sufficently accurate in the frequency band of interest. Futhermore, it should be noted that since PWM signals appear only in the inverter ac output they will only generate radiated EMI to nearby equipment, rather than conducted EMI to the power mains.

b) *di/dt* in the power circuits during commutation among the power switching devices, induce voltage $V=Ldi/dt$ along the parasitic inductances of the commutated circuit and appear as differential mode emissions. In turn this excites the common mode voltages along the parasitic capacitance which then propagates away from the source. The current loop with high *di/dt* will also be an emission source of magnetic field. In high power drive systems, high *di/dt* up to kA/μS can be expected. However, due to relatively small parasitic inductance of tens of nanohenries along the circuit, the induced voltage *Ldi/dt* will be in the range of a only a few volts.

c) *dv/dt* applied to the main circuits by switching action, will certainly directly generate a current *Cdv/dt* persisting during transient periods and appearing in both common mode and differential mode. In practice, drive systems having physically distributed capacitance of a few nanofarads and inductance of a few microhenries would produce a few amperes of pulse transient currents flowing into the power system, which excite noise voltages of over 60 V and result in critical EMI problems. Therefore, in the following sections, the analysis will be concentrated on this type of behavior and its characterization in terms of both the time domain waveform and frequency spectrum.

SIMPLIFICATION OF MODEL TO BE STUDIED

In general, EMI evaluation can be performed with knowledge of only the amplitude of the density function, i.e., the spectrum of the noise sources. As the EMI noise in power electronics is more likely to be pulse train type, they thus can be qualified as broad band noise. There is considerable literature providing essential approaches to evaluation of some typical signals, for instance, the rectangular, trapezoidal, and triangular impulses provided that the waveform

parameters are known [3]. In real power drive systems the EMI signal waveform is very complicated which combines signals generated by different noise sources. However these signals have features in common, e.g., impulse-like and decaying oscillatory behavior. It is useful to first study the waveforms shown as Fig. 1 which were experimentally obtained from a typical motor drive system showing the response ground currents of the motor to a switching action of the inverter. These waveforms clearly feature an impulse decaying oscillatory transient. In motor drive systems it can be experimentally demonstrated that this pulse train current of decaying oscillatory waveform flows from motor and inverter ground wires into the ground network return and back into the inverter through mains. This current pulse occurs during the edge of PWM modulation, e.g. corresponding to a high *dv/dt* instant and is the one of the primary conducted EMI signals in a power drive system. Therefore, for a first approximation three basic models of main circuits responding to power switching *dv/dt* in drive systems are proposed to explain the EMI generating mechanism as follows:

(1) *Second Order Circuit Model*

While circuit dimensions of components are sufficiently small compared with the wavelength of important EMI noise, the distributed parameters of the circuits may be viewed as lumped elements. The motor, as a complex structure which should be treated as a complicated reactance network at radio frequencies [1], may approximately be treated as lumped elements of *L, C,* and *R* whose values will depend on the frequency range. Therefore, a second order circuit, as the simplifying model of main components in drive systems as shown in Fig. 2 may be used to describe the transient behavior.

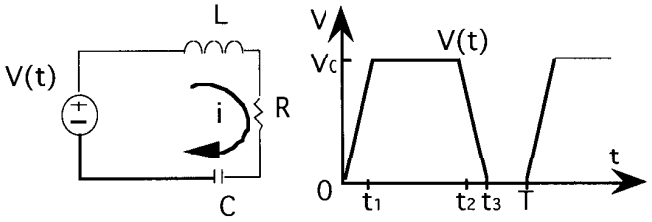

Fig. 2

The power supply and switch device may be described as an equivalent voltage source $V(t)$ having the characteristics of a trapezoidal curve as shown as Fig. 2, where V_0 is the power supply voltage, $\Delta t=t_1$-0 switching time of device, corresponding to the period $(0, t_1)$, (t_2, t_3) and T the repetitive switching period.

One can first solve the second order circuit for current $i(t)$ in the period $(0, t_1)$, e.g. the response to single rise edge of voltage $V(t)$. In the period $(0, t_1)$, we have $V(t)=V't$, $V'=dV/dt$. The KVL equation around the loop is:

$$Ri + L\frac{di}{dt} + \frac{1}{C}\int_0^t idt = V(t) = V't$$

Solving for $i(t)$ with initial conditions $i(0)=0$, $V_c(0)=0$, we have

$$i = CV'[1 - \sqrt{1+(\frac{\beta}{\omega_1})^2}\, e^{-\beta t}\cos(\omega_1 t - \theta)] \qquad (1)$$

where $2\beta=R/L$, $\omega_0^2=1/LC$, $\omega_1^2=\omega_0^2-\beta^2$, and $\tan\theta=\beta/\omega_1$

This result indicates that the current $i(t)$ is an impulse of width $\Delta t=t_1$-0, consisting two component which have amplitude CV', proportional to the change in voltage dV/dt and to the circuit capacitance C. The current waveform clearly depends on Δt and the circuit ω_0. Simulation results of the circuit with different ω_0, shown in Fig. 3 demonstrates a similar waveform when compared with experimental results as shown in Fig. 1.

In the period (t_1, t_2), as $V(t)=V_0$=constant, solving for $i(t)$ with initial conditions $i(0)=i(t_1)$, $V_c(0)=V_c(t_1)$, which can be obtained from the solution of $i(t)$ in the period $(0, t_1)$, we have

$$i = \sqrt{(\frac{V_0 - V_c(t_1)}{\omega_1 L})^2 + i(t_1)^2[1+(\frac{\beta}{\omega_1})^2]}\, e^{-\beta t}\sin(\omega_1 t + \phi) \qquad (2)$$

This is simply a decaying oscillatory current with an amplitude depending on both the initial condition at $t=t_1$, and the supply voltage V_0 , and reactance $\omega_1 L$, lasting a period of about 3 to 4 times of $1/\beta$. The analysis above indicates how the pulse current is produced by the switching along with *dv/dt* and how the parameters of switched circuit will affect the current waveform.

During the period (t_2, t_3), the falling edge of $V(t)$, We may get a similar current with reverse polarity.

One can then proceed to analyze the spectra of the current train while switching repetitively with period $T=1/f_s$ where f_s is the switching frequency of the device. Through Laplace transformation it is then possible to obtain the Fourier transform $F(j\omega)$ of a single pulse current $i(t)$ during rise edge $(0, t_2)$ of $V(t)$. The function $-e^{-j\omega T_3}F(j\omega)$ will correspond to the falling edge (t_2, t_3), where T_3 is the time delay, i.e. the width of the trapezoid. And $F(j\omega)/(1-e^{-j\omega T})$ will be the Fourier transform of a periodic $i(t)$, T is the repetitive period. The Fourier transform of a current pulse train produced by periodic $V(t)$, Fig. 2, will be $F(j\omega)(1-e^{-j\omega T_3})/(1-e^{-j\omega T})$ and its spectrum thus may be expressed as $|F(j\omega)(1-e^{-j\omega T_3})/(1-e^{-j\omega T})|$. We can then apply this process to the known currents, i.e. $i'_1(t)$, $i''_1(t)$ of Eq. (1), and $i_2(t)$ of Eq. (2), to obtain their spectrum respectively [5] ,[6].

a) From $i_1'(t)$, which is a rectangular pulse of width Δt and of amplitude CV', as shown in Eq. (1), with a single pulse,

$$i_1'(t) = CV'u(t) - CV'u(t-\Delta t)$$

where $u(t)$ is step function, we have its Fourier transform as

$$F_1'(j\omega) = CV'\Delta t S_a(\frac{\omega\Delta t}{2}) \qquad (3)$$

where $S_a(\frac{\omega\Delta t}{2}) = \frac{\sin(\frac{\omega\Delta t}{2})}{\frac{\omega\Delta t}{2}}$.

b) From $i''_1(t)$, as shown in Eq.(1), as $\Delta t<<1/\beta$, we assume $e^{-\beta t}=1$, which becomes a gated cosine of width Δt, we have, with a single pulse,

$$i_1''(t) = f_1(t)CV'\sqrt{1+(\frac{\beta}{\omega_1})^2}\cos(\omega_1 t - \theta)$$

where $f_1(t)$ is gated function. Then its Fourier transform is

$$F_1''(j\omega) = CV' \sqrt{1+(\frac{\beta}{\omega_1})^2}\,\frac{\Delta t}{2}[S_a(\omega-\omega_1)+Sa(\omega+\omega_1)] \tag{4}$$

c) From $i_2(t)$, which has the form of a decaying oscillatory signal as shown in Eq. (2), its Fourier transform is

$$F_2(j\omega) = \sqrt{(\frac{V_0 - V_c(t_1)}{\omega_1 L})^2 + i_1(t_1)^2[1+(\frac{\beta}{\omega_1})^2]}\,\frac{\omega_1}{(\beta^2+\omega_1^2-\omega^2)+j2\beta\omega} \tag{5}$$

By use of graphical spectrum analysis examining the change of the envelope of $|F(j\omega)(1-e^{-j\omega T_3})/(1-e^{-j\omega T})|$ from Eq. (3) to Eq. (5), we can obtain useful information concerning the spectrum of the pulse current train which is summarized as follows:

a) Power supply voltage V_0 and the rate of change dv/dt, are each proportional to the amplitude of spectrum.

b) The switching frequency $f_s=1/T$ is approximately proportional to the amplitude of the spectrum.

c) The capacitance C is quite sensitive to the dv/dt producing impulse currents of amplitude CV', having frequency bandwidth $1/\Delta t$ and roll-off rate 20 dB/per decade. Thus, fast, high speed switching definitely produces wide band emissions.

d) Since component $i_2(t)$, the decaying oscillatory waveform lasts a much longer period, because $1/\beta >> \Delta t$, we may conclude that $|F_2(j\omega)|$ dominates the maximum value of the spectrum amplitude over the lower frequency range. The function $|F_2(j\omega)|$ will have a corner frequency of β, and roll-off rate of about 40 dB/per decade.

e) The resonance of the circuit will raise the peak in the spectrum at a resonant frequency ω_1.

f) The pulse width (T_3) modulated waveform of $V(t)$ yields side band signals and spreads the energy density of spectrum comparaed with constant width waveform.

Therefore, the analysis provide a basic concept for understanding the phenomena concerning the responses of motor, semiconductor device, and conductors in power drive system, that produce pulse train during switching operation.

(2) *Transmission Line Model*

A motor drive system usually contains long feeders/cables, the dimensions of which are comparative to the wavelength of the EMI noise. Since the motor is isolated from the ground plane under proposed IEC test conditions [2], a ringing voltage on the motor frame appears and may easily couple to nearby instruments. This effect was observed and is shown in Fig. 4. The ringing frequencies also appear at the emission spectrum as shown as Fig. 4. To explain this behavior it may be supposed that the switching dv/dt is applied to the line feeder, then couples to the ground wire of the motor through the mutual capacitance among wires exciting the standing wave along the ground wire including the motor frame as if it were an open circuit transmission line being excited. The standing wave will absorb current from the power supply. The frequencies which characterize a quarter wave length is equal to the length of the wire. The simulation results of a transmission line of 5.5 meters responding to dv/dt shown as Fig. 5 coincides with this interpretation. The higher the dv/dt or the longer the length of feeder, the larger the excited current will appear. To answer as to when the feeder should be referred to as a transmission line causing EMI problems, we may assume certain criteria concerning whether the wave propagation time delay T_d of the feeder is of close order to the switching time Δt of device. With a far shorter T_d or long Δt, the transmission line effects may be neglected. The simulation results appear to verify this assumption.

(3) *Non-Linear Characteristic Of High Power Rectifier Model*

The rectifier's non-linear characteristic is also one of the major EMI sources in an ac-dc-ac converter. While AC current, including high frequency current flows through the DC bus there will be two kinds of current appearing at the power mains. One is the AC current superimposed on the fundamental load current during diode turn on. The other is due to the AC current being rectified yielding higher order harmonics on the mains while the instantaneous load current is zero.

Another phenomenon is the so called audio-rectification effects due to the modification of the impedance of diodes with respect to a grounded heat sink at the "on-off" frequency. An experimental line current waveform measurement is shown as Fig. 9. As a result of this basis for understanding the EMI noise sources, effective methods of suppression thus can now be developed.

EMI EMISSIONS FROM CONVENTIONAL PWM DRIVES

EMI Measurement Environment For Drive System

According to IEC recommended test procedure for measuring electromagnetic emissions from power drive systems, the schematic diagram of the measurement system is shown in Fig. 6.

a) Equipment Under Test (EUT): a) Inverter, 75 KW, sinusoidal wave control PWM, with IGBTs as main switching devices, 3 phase 460 V 60 Hz input, 3 phase 10-460 V 3-80 Hz output; b) Induction motor, 22.5 KW, 3 phase 460 V 60 Hz, 3500 RPM.

b) Line Impedance Stabilization Network (LISN):

c) Ground plane and ground connection: 2.5 mm aluminum plane with 2x2 meters in size, both inverter and motor are isolated from ground plane while the ground wires of the motor and the drive both are bundled with their three phase power feeders respectively and bonded to ground plane at the ground connection of the LISN.

d) Feeder: 5.5 meters in length for the motor, 1.2 meters for inverter, all of the feeders are placed above the ground plane by at least 0.25 meters.

e) Test conditions: Conducted emission noise measured during inverter motor operating at a frequency at which maximum emissions occur, but with no external mechanical load applied to motor.

Experimental Results of EMI Emissions From Conventional Drive Systems

Fig. 7, Fig. 8, and Fig. 9 show the emission levels in dBμV, emission voltages V_{em} measured at the LISN, line current I_a on the mains. The maximum emission of 125 dBμV occurs at a frequency range of 100 kHz to 200 kHz with roll-off about 20 dB/decade, but then maintaining levels of about 80 dBμV until 20 MHz. The voltage and current wave forms of Fig. 8 and Fig. 9 demonstrate the system response to a switching action.

Explanation of EMI Emissions From Conventional PWM Drives

Every switching operation of the semiconductor devices in the inverter imposes voltage with high dv/dt (about 4 kV/μS for the IGBT devices in this inverter) not only on the line-to-line circuits but also on the line-to-ground circuits. The switched circuits,

usually consist of distributed inductance, capacitance, and resistance, respond to the change in voltage to produce transient currents of wide frequency band flowing into the mains resulting as conducted EMI emissions. The feeder responding to *dv/dt* may produce a standing wave along the feeders resulting in radiated EMI problems. Power rectifier rectification further worsens the emission spectrum.

STRATEGIES FOR EMI REDUCTION

Based upon the analysis of EMI emissions, a set of EMI filters for a 75 KW inverter is shown as Fig. 10 in which the EMI suppression components are small both in size and weight so that they may be readily incorporated with inverter units. A brief explanation of filtering elements is as follows:

a) C_1: These two capacitors were connected as grounding capacitance from both sides of the DC link to the heat sink close to the switching devices and are for compensation of common mode currents flowing from switching devices through parasitic capacitance, including semiconductor to heat sink of switching devices and the load side. The use of C_1 does, however, cause leakage current problems. As in industrial applications power equipment must be well grounded and ground leakage current limit do not apply to such equipment the selection of capacitance C_1 is therefore pertains to an industrial application.

b) C_2: Additional DC bus capacitance was connected across the DC link associated with electrolytic capacitor bank. It compensates for the differential mode noise currents. Because the electrolytic capacitor bank self-resonant frequency is of about 10 kHz, it no longer acts as a capacitance in the high frequency range.

c) C_3: grounding capacitance from the 3-phase input AC mains to the enclosure of the inverter. Capacitance C_3 is utilized for compensation of non-linear effects of the diode rectifier, and audio-rectification effect.

d) L_3 common mode inductance is used for reducing the *dv/dt* of output AC voltage, which, in turn reduces both the transient effects and the magnitude of the motor ground current.

e) L_2: common mode inductance in combination with C_1, C_3 constitutes a second order filter.

f) C_4, L_1, C_5 constitute a third order filter for suppression of the differential mode noise current caused by the non-linear effect of the diode rectifier.

The process of selection of filtering elements for EMI was based on the system EMI noise model and selected by computer simulation. The total weight of these EMI filtering components is less than 5 % of the weight of the high power inverter.

Experimental results of EMI emissions from the same 75 KW commercial inverter drive system are shown in Fig. 11 to Fig. 13, and summarized as follows: a) the maximum emission levels have been suppressed by 55 dB compared with the original drive and down below the CISPR limits by 12 to 15 dB over the entire specified frequency range. b) The motor frame to ground plane voltage ringing has been significantly reduced to one fifth or less. c) Disturbance in the power mains voltage produced by the PWM switching operation has been reduced from 80 Vpeak to 0.5 Vpeak. d) Disturbance in power mains currents by high frequency noise has been reduced to the point where they cannot be easily detected.

CONCLUSION

In PWM drive systems the switching operation along with *dv/dt* is the major cause generating EMI emissions. From an EMI prediction stand point the transient behavior of the system may be described by using a simplified model including a second order circuit model, transmission line model, and non-linear diode model. Based on an proper understanding of noise characteristics of a high power inverter, manufacture of a cost-effective electromagnetic compatible "clean inverter" design is feasible.

AKNOWLEDGMENT

The authors are greatly indebted to the Eaton Corporation and Siei Peterlongo Co. for their support.

REFERENCES

[1] E. Zhong, T.A. Lipo, "Improvements of EMC Performance in Inverter-Fed Motor Drives," IEEE Trans. Ind. Appl. Vol.31 pp.1247-1256 Nov./Dec. 1995.

[2] IEC 22G-WG4 (Cv)9A, "EMC Product Standard Including Specific Testing Methods for Power Systems", March 1994.

[3] Laszlo Tihanyi, Electromagnetic Compatibility in Power Electronics. J.K. Eckert & Company, Inc. Florida,1995.

[4] T.H. Barton, "Pulse Width Modulation Waveforms - the Bessel Approximation," IEEE IAS Conference Proceedings, pp. 1125-1130, 1978.

[5] Richard C. Dorf, Introduction to Electric Circuits. John Wiley & Sons, Inc., New York, 1989.

[6] The Electrical Engineering Handbook. editor-in-chief, Richard C. Dorf, CRC Press, Inc. Florida, 1993.

[7] Clayton R. Paul, "Solution of the Transmission-Line Equations for Three-Conductor Lines in Homogeneous Media," IEEE Trans. EMC. Vol. EMC-20, No. 1, February 1978.

[8] M. Nave, Power Line Filter Design for Switching-Mode Power Supplies. Van Nostrand Reinhold, New York 1991.

[9] J.C. Fluke,Sr. Controlling Conducted Emissions by Design. Van Nostrand Reinhold, New York 1991.

[10] R. Lee Ozenbaugh, EMI Filter Deaign. Marcel Dekker, Inc. New York 1995.

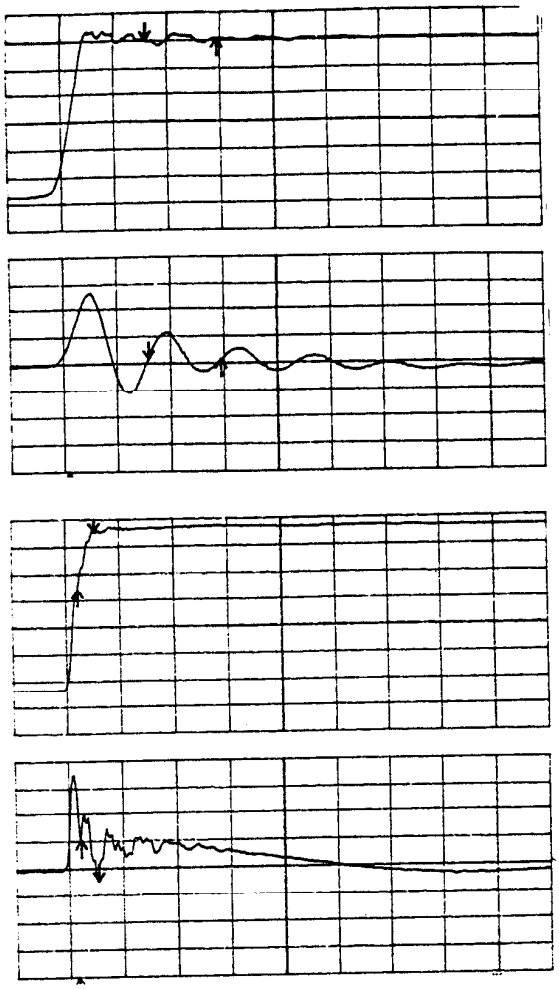

Fig. 1 Motor Line-to-Frame Voltage and Frame-to-Ground Current Ig
a) 22.5 KW motor with 5.5 meter feeders,
100 V/div, 2 A/div , 0.5 μS/div
b) 2 KW motor with 0. 5 meter feeders,
100 V/div, 0.2 A/div, 0.5 μS/div

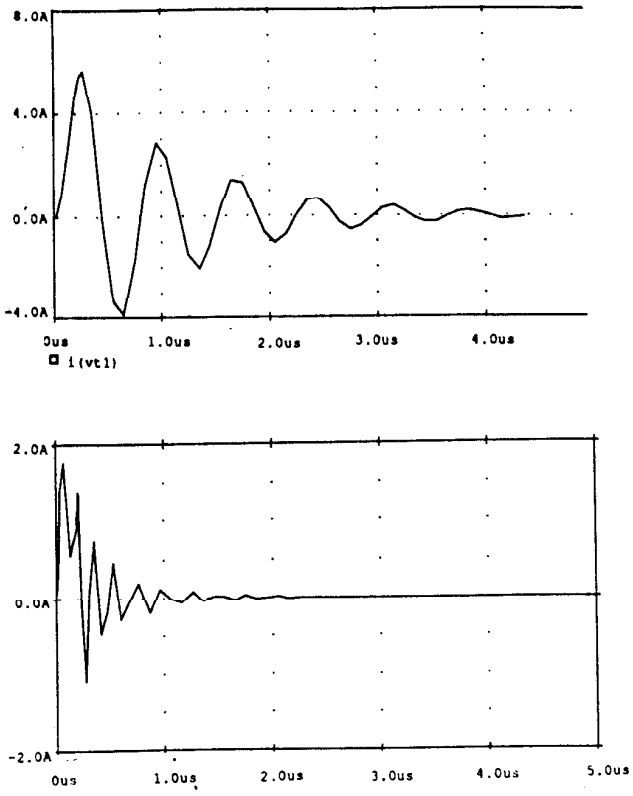

Fig. 3 Second Order Circuit Response Current
---- Simulation results
dv/dt=700 V/0.2 μS
a) L=9 μH, C= 1.2 nF, R=20 Ω
b) L=0.9 μH, C= 0.3 nF, R=10 Ω

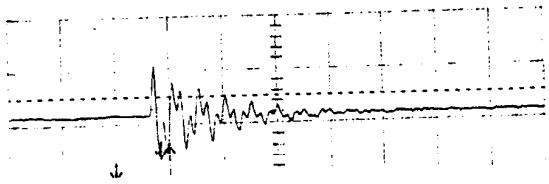

Motor Frame-to-Ground Voltage
TR1 200 V/div, 1 μS/div

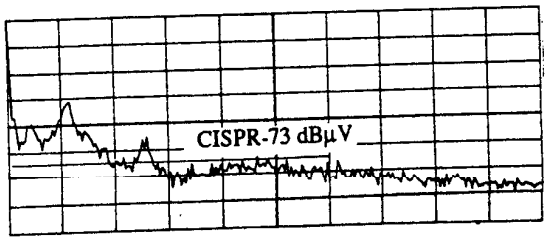

Fig. 4 Emission Levels From 15 KW Drive
Rev 127 dBμV, 10 dB/div
TR2 5 MHz/div, 0-50 MHz

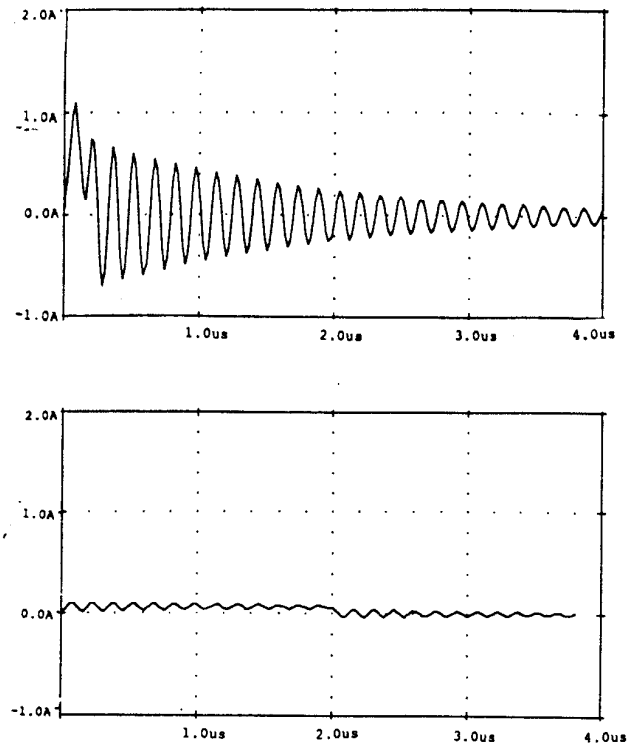

Fig. 5 Transmission Line Current Responding to dv/dt
----Simulation Results
a) dv/dt 700 V/0.2 μS, line Td=38 nS 220 Ω
b) dv/dt 700 V/2 μS, line Td=38 nS 220Ω

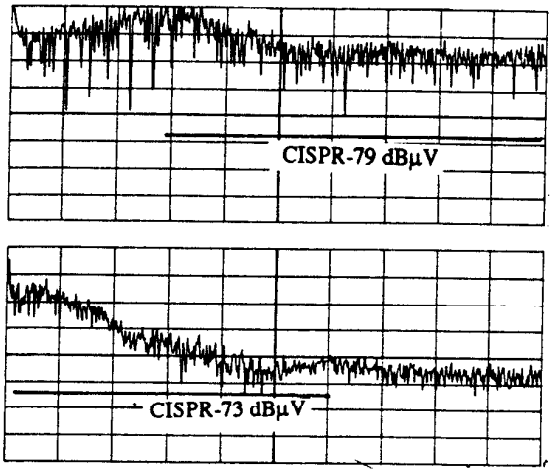

Fig. 7 Emission Levels (Vem) From Conventional 75 KW Drive System Feeding 22.5 KW Induction Motor
Rev. 127 dBμV, 10 dB/div
TR1 frequency 50 kHz/div, 0 to 500 kHz
TR2 frequency 5 MHz/div, 0 to 50 MHz

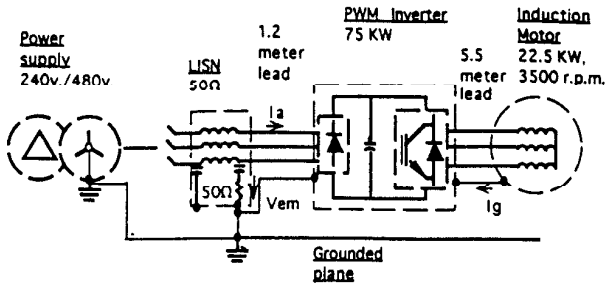

Fig. 6 Measurement of Conducted Radio Noise Emissions from Inverter-Fed Motor Drive

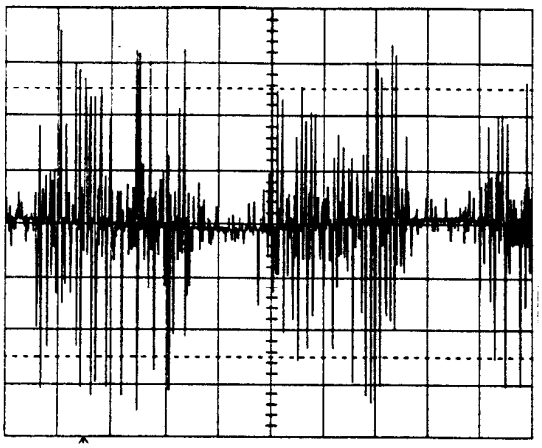

Fig. 8 Emission Voltage (Vem) Waveform From Conventional 75 KW Drive System Feeding 22.5 KW Induction Motor
V/div 20 V, Time/div 2 mS

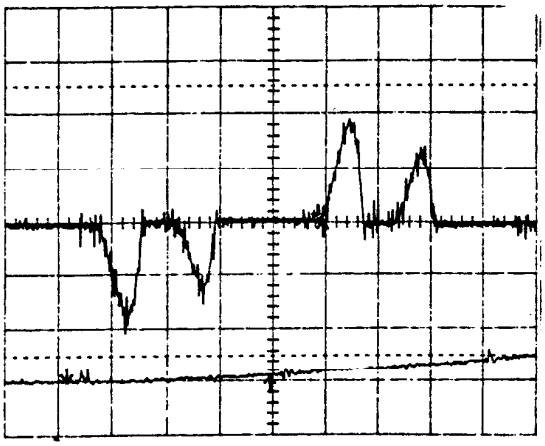

Fig. 9 Mains Current (Ia) From Conventional 75 KW Drive System Feeding 22.5 KW Induction Motor
A/div 5 A, Time/div 2 mS

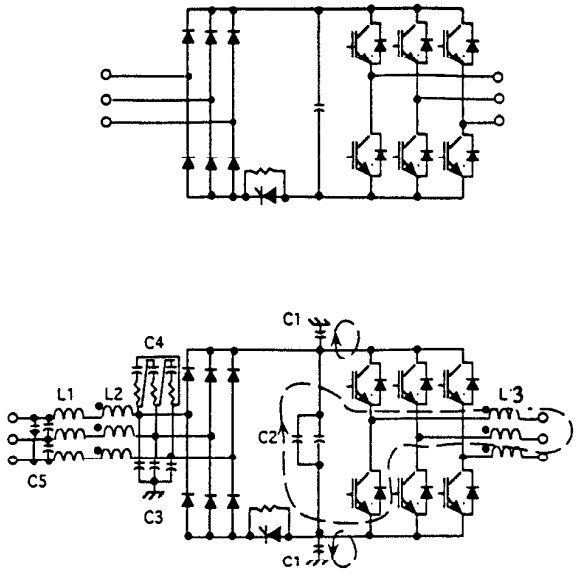

Fig. 10 Main Circuit of 75 KW Inverter
a) Conventional Configuration
b) With EMI Filter Components

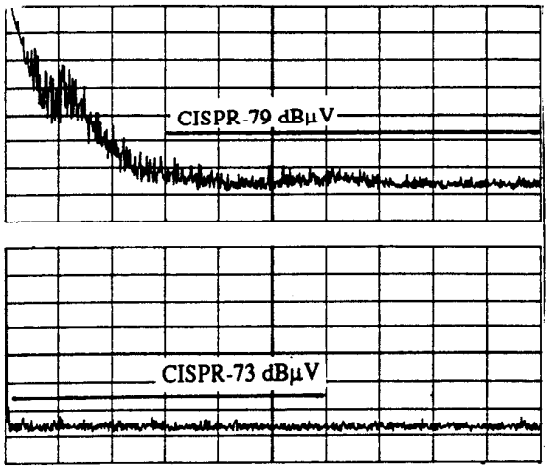

Fig. 11 Emission Levels From 75 KW Drive System Feeding 22.5 KW Induction Motor, with EMI Filter Components
Rev. 127 dBμV, 10 dB/div
TR1 frequency 50 kHz/div, 0 to 500 kHz
TR2 frequency 5 MHz/div, 0 to 50 MHz

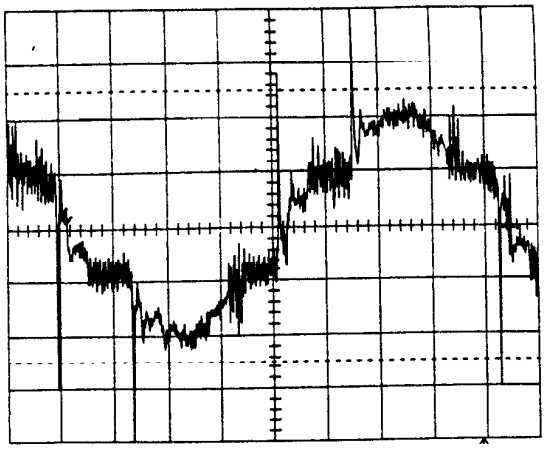

Fig. 12 Emission Voltage Waveform from 75 KW Drive System Feeding 22.5 KW Induction Motor, with EMI Filter Components
V/div 1 V, Time/div 2 mS

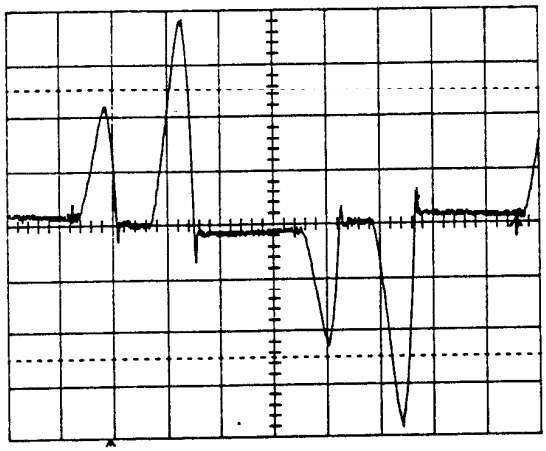

Fig. 13 Mains Current From Conventional 75 KW Drive System Feeding 22.5 KW Induction Motor, with EMI Filter Components
A/div 5 A, Time/div 2 mS